Desalination and Water Treatment
www.deswater.com
9 (2009) 96–104
1944-3994/1944-3986

Development of a hybrid solar distillator of a basin type distillator and a membrane distillator

K. Murase[a,*], Y. Yamagishi[a], K. Tano[a]

[a]*Department of Applied Chemistry, Faculty of Science and Engineering, Chuo University, 1-13-27, Kasuga, Bunkyo-ku, Tokyo, Japan*
Tel. +81(3)3817-1912; Fax. +81(3)3817-1895; email: hmurase@kc.chuo-u.ac.jp

Received 15 September 2008; Accepted 29 March 2009

ABSTRACT

A tube-type solar distillator hybridized a conventional basin still with an air-gap membrane distillator using PTFE membrane was numerically and experimentally investigated for drinking water or irrigation. A tube-type basin still is directly combined with a flat-type membrane distillator through an absorber for solar irradiation within the distillator. Membrane distillation enables water to flow under an absorber at the stable state and water vapor to transfer in the downward direction due to support of membrane. Distillate productivity in case of a bilateral water feeding operation at the steady state almost equals to the summation of productivity in case of one-way feeding method independently for basin still and membrane distillator. The numerical simulation revealed that membrane distillation mostly produced distillate water at the range of low solar irradiation and basin distillation contributed to productivity at the high irradiation. Dynamic characteristics of the hybrid distillator were investigated in the indoor laboratory by using a meteorological data in Japan. The distillate per a day was produced to be 2.18 kg/(m^2 · day) at an irradiative intensity of lamps per a day, 22.6 MJ/(m^2 · day).

The hybrid solar distillator will contribute to enhance distillate productivity for practical use.

Keywords: Hybrid solar distillator; Membrane distillation; PTFE membrane; Basin still

1. Introduction

Arid regions have been year by year expanding in the world with drastic increases in industrialization. Desalination technologies considerably contribute not only to the shortage theme of water resources but also to such an environmental problem as global warming by means of irrigation. Solar distillation system is one of the best solutions for remote areas or arid regions with the lack of water due to the utility of free energy and clean environment. However, the weak point of the low water productivity of solar distillation leads to research activities for the development of a variety of solar still devices and processes as reviewed in references [1–5].

On the other hands, membrane distillation (MD) is a desalting process that is coupling conventional distillation with membrane separation. MD is a membrane technique for separating water vapor from saline water through the pores of such a hydrophobic membrane as PTFE (PolyTetraFluoroEthylene) sheet. The advantages of MD compared to other pressure-driven separation processes such as reverse osmosis, ultrafiltration and microfiltration result from the high selectivity, lower operating temperature or pressure and the high-mass transfer rate in references [6, 7]. B.V.Bruggen et al. [8] overviewed the comparison between distillation and membrane filtration processes in seawater desalination. However, one of the most serious issues for the practical use is to secure the energy source for distillation. The low thermal driven processes in membrane

*Corresponding author.

Presented at the Conference on Membranes in Drinking and Industrial Water Production, 20–24 October 2008, Toulouse, France.

distillation are appropriate for the utilization of solar energy. Membrane distillation processes driven by solar energy has been investigated as the low cost, energy saving processes [9–12]. The effective idea for the enhanced distillate productivity is development of an integrated [13] or a hybrid solar distillator.

A networked system of tube-type solar stills combined with solar ponds has been proposed for use in the desert environment [14, 15]. In a conventional basin-type solar still, the only upward transfer of evaporated vapor from the basin to a cover results in a factor of the low productivity due to the decrease of temperature difference between brine and a cover. The downward heat flow against gravity contributes to an energy-free process for heating and cooling operation in MD. A variety of methods in MD are classified into four categories; direct contact membrane distillator (DCMD), air gap membrane distillator (AGMD), vacuum membrane distillator (VMD) and sweeping gas membrane distillator (SGMD) [16]. AGMD is the most appropriate method for a solar distillator due to the low conductive heat loss from evaporated water to distillate water. The direction of vapor transfer in AGMD depends on the setup of the distillator due to support of liquid film by a membrane. The hybridization of a basin-type distillator with AGMD contributes to the effective utilization for solar energy due to the bilateral vapor transfers, that is upward and down ward direction against gravity. Our developed hybrid solar distillator is a tube-type basin distillator combined with a flat-type AGMD through an absorber for solar irradiation.

This paper presents the fundamental specifications of a hybrid solar distillator. For evaluating effects of hybridization on distillate productivity, the static and dynamic characteristics were verified experimentally on the indoor conditions and numerically by using the simple simulation model. Heat and mass transfers in a basin still [1, 3, 17] and AGMD [18–23] have been numerically estimated. The experimental and numerical analyses reveal us to be the synergistic effect of basin and membrane distillation.

2. Experimental set-up

Figure 1 shows the schematic cross section of a tube-type hybrid solar distillator. This hybrid module located horizontally at the central plane of a pylex glass tube is directly combined to a basin-type of solar still with a flat-type of membrane distillator using PTFE (PolyTe traFluoroEthylene) membrane. The absorber for solar irradiation, which is made of a black-painted aluminum plate for enhancement of absorbability, splits up the space into saline waters for basin distillator and membrane distillator. The membrane distillator composes of a aluminum absorber (2 mm in thickness), feeding water (2mm in thickness), PTFE membrane (NITTO-DENKO Co. Ltd., NTF-5200, 1 μm in pore diameter, 85 μm in thickness and 80% in void fraction), a vapor diffusion gap supported with fine and coarse types of polyethylene meshes (5 mm in thickness) and a aluminum radiator (2 mm in thickness). The water depth in a basin is kept to be a constant, 10 mm. Solar energy absorbed through a glass cover heats up two feeding waters over and under the absorber. On the one hand vapor evaporated in basin distillator diffuses in the upward direction from the basin into the outer glass cover, on the other hand vapor evaporated in membrane distillator transfers in the downward direction from water partition into the bottom plate of distillator. This hybrid distillator effectively utilizes the spaces of vapor transfer within it.

The effective size of a module is 0.70 m in length, 0.08 m in width. The size of the distillator is 0.75 m in length, 0.14 m in width. The inclination of the hybrid distillator is fixed at 5 degree for flowing down distillate water in basin still along the glass cover, but the module is kept at the horizontal level for the constant depth of water in basin distillator. Several drain tubes are equipped on the radiator for the more effectively discharge of distillate water in membrane distillator. Experimental data were measured in the indoor laboratory by using infrared lamps. Irradiative intensity of lamps was adjusted by volt-sliders in the range from 200W/m^2 to 800W/m^2, which was calibrated with by pyranometer (EKO Instruments Co. LTD. Model MS-42). Irradiative intensity of infrared lamps was stepwise changed for a day according to a characteristic meteorological data in Japan [15] in order to evaluate the dynamic characteristics

Distillated water was used for the purpose of estimating static and dynamic characteristics of the distillator. Cupper and constantan thermocouples are attached on several points marked with dots in Fig. 1. Feeding water is separately supplied into two partitions of basin and membrane distillator stably at the constant water pressure by two head tanks.

In order to evaluate the hybridization at the steady state, the following three operations were investigated:

1. No feeding in membrane distillator for estimating the distillate productivity in basin still.
2. No feeding in basin still for estimating the distillate productivity in membrane distillator.
3. Feeding direction from membrane distillator to basin still in hybrid distillator.

3. Numerical simulation

3.1. Heat and mass balances

Figure 2 shows the simulated model for a hybrid distillator. The tubular glass cover is modeled as such a flat

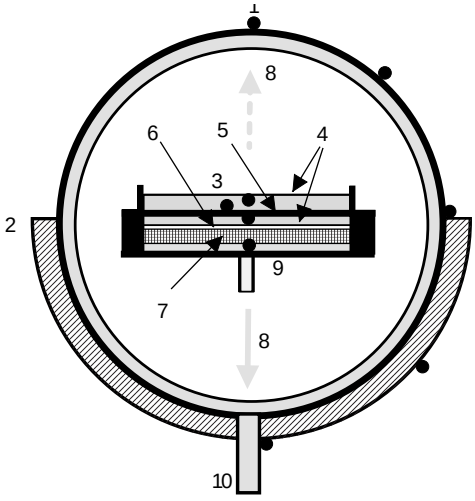

1. Pyrex glass tube
2. Half-cut gray PVC tube
3. Basin still
4. Saline water
5. Absorber for solar irradiation
6. PTFE membrane
7. Polyethylene mesh spacer
8. distillated water
9. Radiator
10. Drain tube for disltillated water

Red area : Heated water
Blue area : Distillated water
Measured points of thermocouples

Fig. 1. A schematic diagram of a tube-type hybrid solar distillatory.

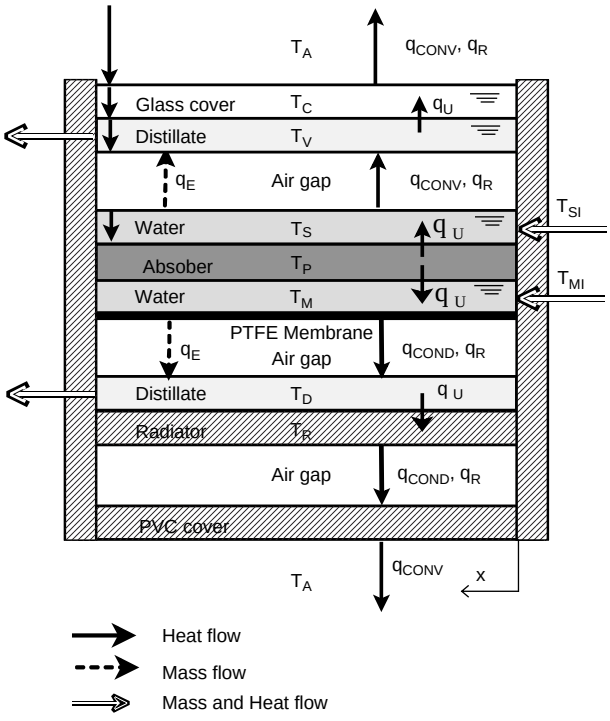

Fig. 2. Heat and mass transfer model for a tube-type hybrid distillatory.

plate as the module in order to establish a one-dimensional model [24, 25]. The interval between a hybrid module and a cover is approximated by the half radius of a glass tube.

The following assumptions were made in order to take mass and heat balances:

1. Temperature gradients across various partitions are negligible.
2. Temperature polarization across the PTFE membrane is negligible.
3. Distillate productivities in basin and membrane distillator are independently calculated
4. Natural convection occurs only within the space over the basin still due to the temperature gradient.
5. The mesh spacer within the air gap between the PTFE membrane and the radiator has no effect on the heat and mass transfer.

Energy balances for some partition at the steady state under the above assumptions are presented as follows:

Glass cover:

$$0 = k_C \Gamma \frac{d^2 T_C}{dx^2} + \left(\alpha_C I + q_{U,VC}\right) - \left(q_{CONV,CA} + q_{R,CS}\right) \tag{1}$$

Distillate in basin still:

$$\rho_V C_{P,V} u_V \Gamma \frac{dT_V}{dx} = k_V \Gamma \frac{d^2 T_V}{dx^2} + \left(\alpha_V \tau_C I + q_{E,SV} + q_{CONV,SV} + q_{R,SV}\right) - \left(q_{U,VC}\right) \tag{2}$$

Water in basin distillator:

$$\rho_S C_{P,S} u_S \Gamma \frac{dT_S}{dx} = k_S \Gamma \frac{d^2 T_S}{dx^2} + \left(\alpha_S \tau_C \tau_V I + q_{U,PS}\right) - \left(q_{E,SV} + q_{CONV,SV} + q_{R,SV}\right) \tag{3}$$

Absorber:

$$0 = k_P \Gamma \frac{d^2 T_P}{dx^2} + \left(\alpha_P \tau_C \tau_V \tau_S I\right) - \left(q_{U,PS} + q_{U,PM}\right) \tag{4}$$

Water in membrane distillator:

$$\rho_M C_{P,M} u_M \Gamma \frac{dT_M}{dx} = k_M \Gamma \frac{d^2 T_M}{dx^2} + \left(q_{U,PM}\right) - \left(q_{E,MD} + q_{COND,MD} + q_{R,MD}\right) \tag{5}$$

Distillate in membrane distillator:

$$\rho_D C_{P,D} u_D \Gamma \frac{dT_D}{dx} = k_D \Gamma \frac{d^2 T_D}{dx^2} + \left(q_{E,MD} + q_{COND,MD} + q_{R,MD}\right) - \left(q_{U,DR}\right) \tag{6}$$

Bottom plate of hybrid distillator (Radiator):

$$0 = k_R \Gamma \frac{d^2 T_R}{dx^2} + \left(q_{U,DR}\right) - \left(q_{COND,RB} + q_{R,RB}\right) \quad (7)$$

PVC Cover:

$$0 = k_B \Gamma \frac{d^2 T_B}{dx^2} + \left(q_{COND,RB} + q_{R,RB}\right) - \left(q_{CONV,BA}\right) \quad (8)$$

Physical properties and heat transfer coefficients in equations.(1)–(8) are list up in appendix.

The above differential Eqs. (1)–(8) were numerically analyzed under the boundary conditions as follows:

Boundary Conditions

(I) inlet (at x=0)

a) $$\frac{dT_C}{dx} = \frac{dT_V}{dx} = \frac{dT_P}{dx} = \frac{dT_D}{dx} = \frac{dT_R}{dx} = \frac{dT_B}{dx} = 0 \text{ ; adiabatic condition} \quad (9)$$

b) $$T_S(0) = T_{S,Inlet}, T_M(0) = T_{M,Inlet} \text{ ; inlet flow condition c} \quad (10)$$

(II) outlet (at x=L)

a) $$\frac{dT_C}{dx} = \frac{dT_P}{dx} = \frac{dT_R}{dx} = \frac{dT_B}{dx} = 0 \text{ ; adiabatic condition} \quad (11)$$

b) $$q(L) = q_{E,V}, q(L) = q_{E,S}, q(L) = q_{E,D} \text{ ; outlet sensible heat flux} \quad (12)$$

Distillates in basin and membrane distillator are respectively estimated as follows [24, 25]:

Distillate in basin distillator [3]

$$D_{Basin} = \frac{(16.273 \times 10^{-3}) h_{CONV,SV} \left(P_S - P_V\right)}{\lambda}, h_{CONV,SV} = 0.884 \left[\left(T_S - T_V\right) + \frac{\left(P_S - P_V\right) T_S}{\left(268.9 \times 10^3 - P_S\right)} \right]^{1/3} \quad (13)$$

Distillate in membrane distillator [26]

$$D_{Membrane} = \frac{D}{A} \frac{1}{\left(\delta / \zeta^{3.6} + z\right)} \frac{\left(P_S - P_D\right)}{P_{BM}}, = \frac{RT}{\pi} \quad (14)$$

Total distillate productivity is estimated by using the summation of Eqs. (13)–(14).

Total distillate productivity $D = D_{Basin} + D_{Membrane}$ (15)

3.2. Numerical procedure

In order to numerically integrate differential Eqs. (1)–(8) under boundary conditions (9)–(12), Galerkin finite element method was applied for the energy balances by using the one-dimensional biquadratic shape function for temperature. The computational domain was discretized into 30 elements in the flow direction. Unknown temperature variables at node points were numerically evaluated with a iteration process until under 0.1% relative error.

4. Results and discussion

4.1. Static characteristics

4.1.1. Distillate productivity

Figure 3 shows the effect of irradiative intensity of lamps on distillate productivity at steady state in experimental case of feeding only for basin destination (EXP-BASIN), feeding only for membrane destination (EXP-MEMBRANE), feeding for hybrid destination (EXP-HYBRID), the summation of productivity EXP-BASIN and EXP-MEMBRANE, the corresponding tube-type solar still with a half-cut tube basin still in reference [14] and in numerical case of hybrid distillator (CAL-HYBRID). The productivity in filled marked circles (EXP-HYBRID) almost equals to that in blank circles, namely the summation of distillates by basin destination (EXP-BASIN) and membrane destination (EXP-MEMBRANE). The hybridization of basin and membrane destination at the steady state results in the corresponding effect of each solo module in spite of the increased heat capacity of a hybrid distillator. The simulation model overestimates productivity at the range of the high irradiative

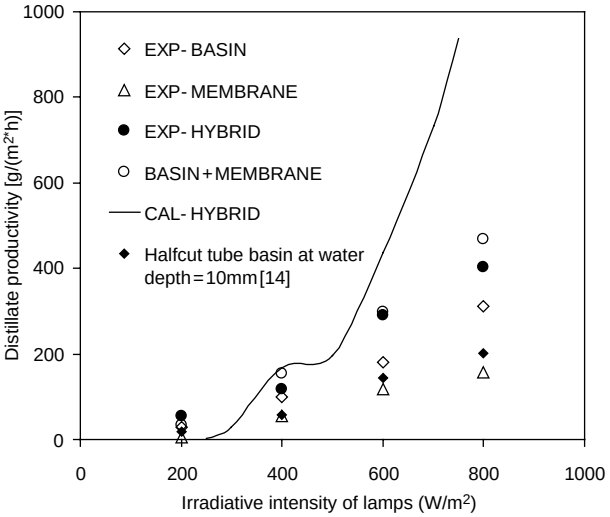

Fig. 3. Effect of irradiative intensity of lamps on distillate productivity in cases of (1) only basin distillation (EXP-BASIN), (2) only membrane distillation (EXP-MEMBRANE), (3) hybrid distillation (EXP-HYBRID), (4) summation of case(1)+(2), (5) numerical simulation (CAL-HYBRID) (6) half-cut tube basin still in reference [14](water depth=10mm).

intensity over 400W/m^2 and underestimates at the low irradiative intensity below it rather than that in experiment. This error around at irradiative intensity, 400W/m^2, closely interrelates with the unexpected increased productivity. The degree of thermal resistances of waters in basin and membrane distillator determined the transfer direction of absorbed energy. The depth of water in basin still equals to the five times depth of water in membrane distillator.

4.1.2. Relative distillate productivity

In order to analyze the unexpected simulated productivity around at 400W/m^2 in Figure 3, each distillate in basin and membrane distillation evaluated respectively by using equations (13), (14) is indicated in Figs. 4 (a)–(d) with the relative distillate along the displacement from the inlet to the maximum distillate. Figure 4-c indicates that the intensity, 550W/m^2, is the critical value for the absorbed energy due to the equivalent productivity in both cases of basin and membrane distillation. Distillate produced by membrane at the range of the lower intensity than 550W/m^2 is larger than that by basin. The total distillate at 400W/m^2 is equal to that only by membrane distillation in Fig. 4(a). The higher temperature difference between water surface and bottom plate of module contributes to the higher productivity. The lower productivity by membrane distillation at the range of the high irradiative intensity is stemmed from the saturated gap of vapor diffusion due to the heat loss by thermal conduction. On the other hands, the narrow gap and the shallow water depth contribute to the effective performance of distillate at the low range of irradiative energy due to the lower heat capacity in spite of the low driving force that is the small temperature difference.

4.1.3. Simulated temperature profiles

Figures 5 (a) and (b) show numerical temperature profiles along displacement from the water inlet at the irradiative intensity, 400W/m^2 and 600W/m^2 in order to verify the dependence of irradiative intensity on

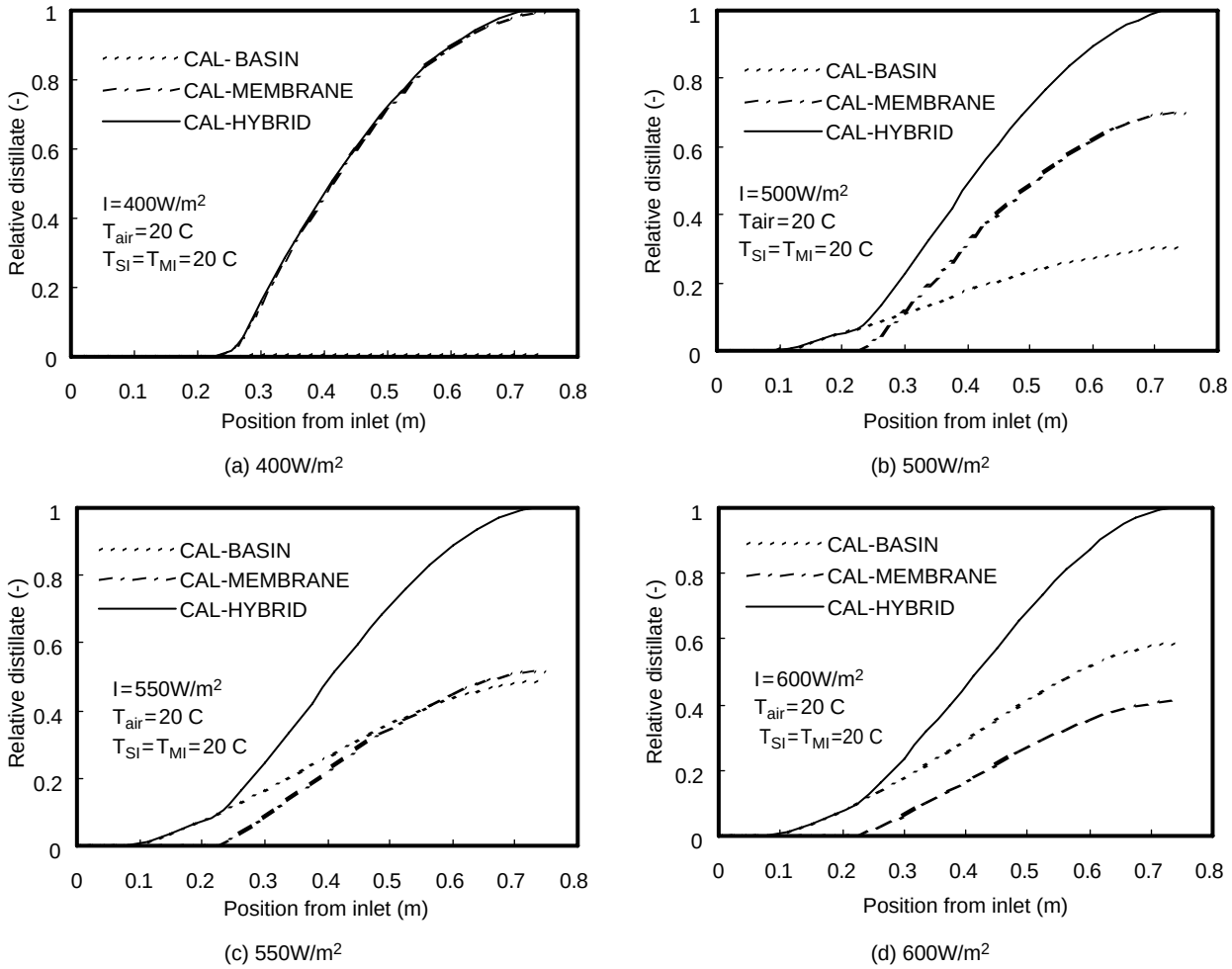

Fig. 4. Profiles of relative distillate productivity along displacement from inlet (x = 0) to the maximum distillate.

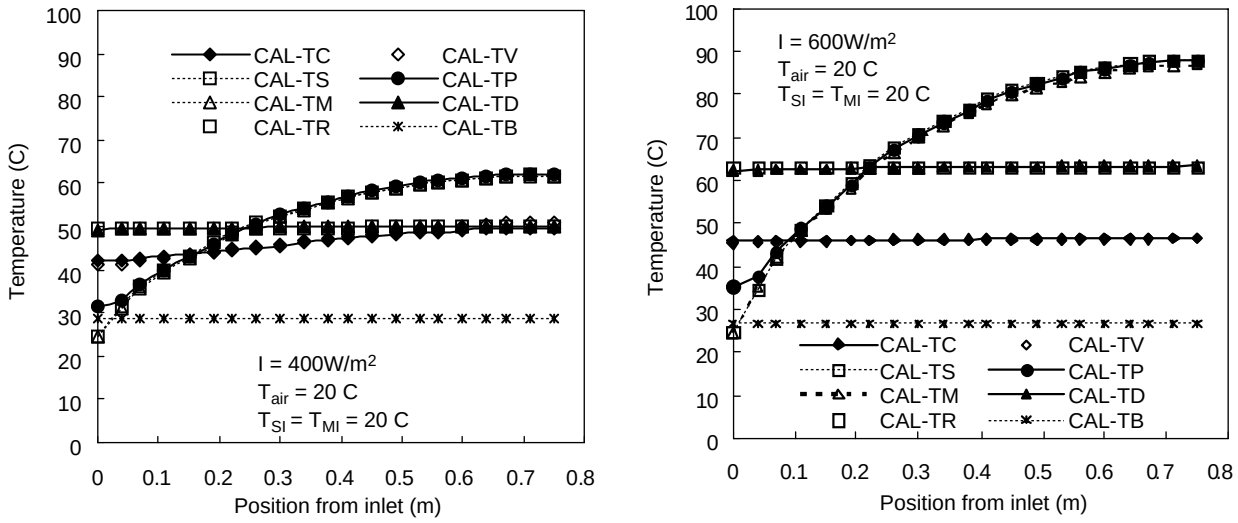

(a) 400W/m^2 (b) 600W/m^2

Fig. 5. Temperature profiles along the position from inlet of feed.

the peculiar productivity in hybrid distillator. Figure 5 (b) indicates the constant temperature difference between a glass cover and feed in basin still although the temperature difference at 400W/m^2 decrease along displacement from inlet in Fig. 5 (a). The convective heat transfer coefficient between water and a glass cover, $h_{CONV,\,SV}$ contributes to the result.

4.1.4. Averaged temperature

In order to compare measured temperatures with numerical ones, averaged temperatures of partitions along the distillator are plotted in Figs. 6 (a) and (b) at the irradiative intensity, 400W/m^2 and 600W/m^2. Experimental data with blank triangles are measured in hybrid distillator without water in the basin. Simulated data have good agreements with experimental data at the low range of irradiative intensity, 400W/m^2. Cover temperature at 600W/m^2 is numerically underestimated but water or absorber temperature within hybrid distillator is reversely overestimated. These result in the overestimation of distillate productivity stemmed from the temperature difference. One of error factors is due to evaluate the conventional interrelationship of the convective heat transfer coefficient because the actual convective space, a half round shape, is approximated by a rectangular one.

4.2. Dynamic characteristics

Dynamic characteristics of the hybrid distillator are evaluated in Figs. 7 (a) and (b) by using a simulated meteorological data in Japan, Sept. 3, 2006 [15]. Each

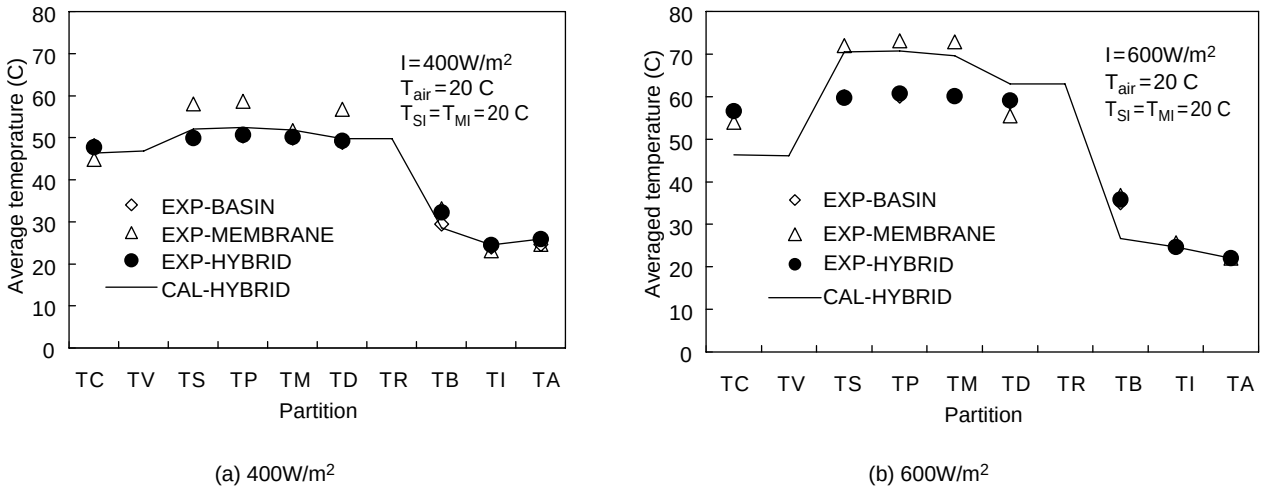

(a) 400W/m^2 (b) 600W/m^2

Fig. 6. Average temperature of partitions along displacement from inlet.

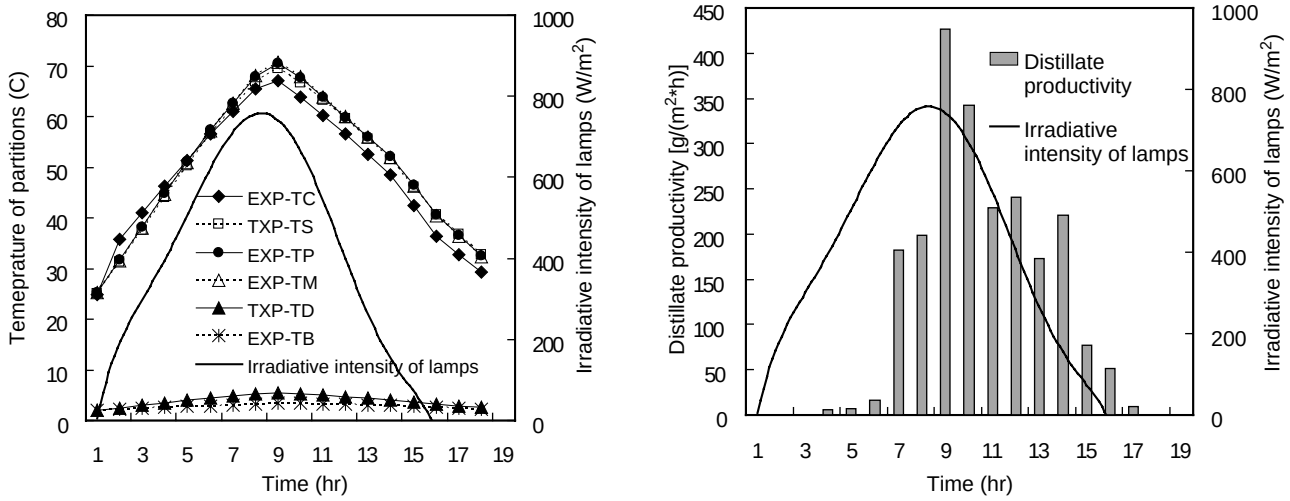

(a) Time elapses of partitions temperatures

(b) Time elapses of distillate productivity

Fig. 7. Dynamic characteristics of distillate productivity for one day.

temperature of partitions gradually decreases after the peak of solar irradiation due to the high heat capacity of hybrid distillator in spite of the low temperature of the PVC cover. On the other hand, the time response of productivity is insensitive for the irradiative intensity until the peak value. Moreover, the effect of heat accumulation is not expected due to the same ending time of intensity and productivity. The small inclination of hybrid distillator interrupts the smooth drain of distillate water on the radiator.

The distillate productivity per a day is obtained to be 2.18kg/(m^2 · day) at the irradiative intensity per a day, 2.6MJ/(m^2 · day) This productivity is almost equivalent to with the performance of a tube-type solar still with heat accumulator [15]. Feeding water into the hybrid distillator is supplied independently into the basin and membrane partitions. The skillful idea for the drain of distillate in membrane distillation or an optimal operation for feed, counter or parallel flow, expectedly will contribute to the enhanced distillate productivity.

5. Conclusions

A tube-type hybrid solar distillator with a conventional basin still and an air-gap membrane distillator by using PTFE membrane was numerically and experimentally investigated for drinking water or irrigation. A tube-type basin still is directly combined with a flat-type membrane distillator through an absorber for solar irradiation within the distillator. The fundamental static and dynamic characteristics were revealed as follows,

1. Distillate productivity in case of a bilateral water feeding operation at the steady state almost equals to the summation of productivity in case of one-way feeding method independently for basin still and membrane distillation.
2. The numerical simulation revealed that membrane distillation mainly produces distillate water at the range of low solar irradiation and basin distillation contributes to productivity at the high radiation.
3. Dynamic characteristics of the hybrid distillator were investigated in the indoor laboratory by using a meteorological data in Japan. The distillate per a day was produced to be 2.18kg/(m^2 · day) at a irradiative intensity per a day, 22.6MJ/(m^2 · day).

Water flowed into the hybrid distillator is supplied independently into the basin still and membrane distillator in this experiment. The skillful idea for the drain of distillate in membrane distillation or an optimal operation for feed, counter or parallel flow, expectedly will contribute to the enhanced distillate productivity.

Nomenclature

C_P	: Specific heat	[J · kg^{-1} · K^{-1}]
D	: Distillate productivity	[kg · m^{-2} · s^{-1}]
D	: Diffusion coefficient of vapor into air	[ms^{-2}]
e	: Porosity of PTFE membrane	[–]
h_{COND}	: Conductive heat transfer coefficient	[W · m^{-2} · K^{-1}]
h_{CONV}	: Convective heat transfer coefficient	[W · m^{-2} · K^{-1}]
h_E	: Evaporative heat transfer coefficient	[W · m^{-2} · K^{-1}]
h_E	: Radiative transfer coefficient	[W · m^{-2} · K^{-1}]

I : Solar intensity [W · m^{-2} · K^{-1}]
k : Thermal conductivity [W · m^{-1} · K^{-1}]
l : Thickness of partition [m]
L : Length of hybrid distillator [m]
P : Saturated vapor pressure [Pa]
P_{BM} : Logarithmic average [Pa]
q_{COND} : Conductive heat flux: $q_{COND,AB} = h_{COND,AB}(T_A - T_B)$ [W · m^{-2}]
q_{CONV} : Convective heat flux: $q_{CONV,AB} = h_{CONV,AB}(T_A - T_B)$ [W · m^{-2}]
q_E : Evaporative heat flux $q_{E,AB} = h_{E,AB}(T_A - T_B)$ [W · m^{-2}]
q_R : Radiative heat flux $q_{R,AB} = h_{R,AB}(T_A - T_B)$ [W · m^{-2}]
q_U : Overall heat flux $q_{U,AB} = h_{U,AB}(T_A - T_B)$ [W · m^{-2}]
R : Gas constant [J · mol^{-1} · K^{-1}]
T : Temperature [K]
u : Flow velocity [m/s]
U : Overall heat transfer coefficient [W · m^{-2} · K^{-1}]
V : Wind velocity [m · s^{-1}]
x : Distance from feed [m]
Z : Interval between membrane and condensate plate [m]

Subscripts

AV : Average
B : PVC(polyvinyl chloride) cover
C : Pylex glass cover
D : Distillate in membrane distillator
M : Brine in membrane distiilator
P : Absorber
S : Brine in basin still
R : Condensate plate
V : Distillate in basin still
BA : between PVC cover and air
CA : between pylex glass cover and air
CS : between pylex glass cover and sky
DR : between pylex glass cover and sky
MD : between brine and distillate in membrane distillator
PM : between absorber and Brine in membrane distillator
PS : between absorber and brine in basin still
RB : between condensate in membrane distillator and PVC cover
SV : between brine in basin still and distillate in basin still
VC : between distillate in basin still and pylex glass cover
COND : Conductive heat transfer
CONV : Convective heat transfer

Greek

α : Absorptivity of partition [–]
γ : Reflectivity of partition [–]
ε : Emissivity of partition [–]
τ : Transmissivity of partition [–]
λ : Latent heat of water [kJ/kg]
ρ : Density [kg/m^3]
σ : Stefan-Boltzman constant [W/(m^2 · K^4)]
ϕ : Overall absorptivity of radiation [–]
η : Thermal efficiency [–]
π : Total pressure(atmospheric pressure) [Pa]
δ : Membrane thickness [m]
Γ : Width of hybrid distillator [m]

Appendix

The approximate equations for heat transfer coefficients are as follows [3, 24]:

Thermal conductivities

$$k_C = 1.3, k_V = k_S = k_M = k_D = 0.602, k_P = 200, k_B = 0.151 W/(m \cdot K), \quad \text{(A-1)}$$

Thermal conductivity of air

$$k_A = 0.0244 + 0.7673 \times 10^{-4} T_A, W/(m \cdot K) \quad \text{(A-2)}$$

Sky Temperature

$$T_{sky} = T_A(0.55 + 0.06548\sqrt{fP_A}), K \quad \text{(A-3)}$$

Absorptivity of solar absorber and water

$$\alpha_C = 0.85, \alpha_V = \alpha_S = 0.82, \alpha_P = 0.95, \tau_C = \tau_V = \tau_S = 0.92 \quad \text{(A-4)}$$

Overall absorptivity

$$1/\phi_{12} = 1/\varepsilon_1 + 1/\varepsilon_2 - 1 \quad \text{(A-5)}$$

Latent heat of water

$$\lambda_V = \lambda_D = 2.3246 \times 10^3 (1.0727 \times 10^3 - 1.0167T + 1.4087 \times 10^{-4} T^2 - 5.1462 \times 10^{-6} T^3, J/kg \quad \text{(A-6)}$$

Heat capacity of saline water

$$C_S = C_M = (4.2055 - 0.0678S + 1.4757 \times 10^{-3} S^2) \times 10^3 - (13.604 - 6.1917S + 0.3251S^2) \times 10^2 T + (15.908 - 5.0572S + 0.2562S^2) \times 10^{-3} T^2, J/(kg \cdot K)$$
$$C_C = 0.77 \times 10^3, C_V = C_D = 4.18, C_B = 1.0 \times 10^3 \quad \text{(A-7)}$$

Conductive heat transfer coefficient

$$h_{COND,MD} = \frac{k_A}{\ell_{MD}}, h_{COND,RB} = \frac{k_A}{\ell_{RB}} \quad \text{(A-8)}$$

Convective heat transfer coefficient

$$h_{CONV,CA} = h_{CONV,BA} = 5.7 + 3.8 \times V,$$
$$h_{CONV,SV} = 0.884 \left[T_S - T_V + \frac{(P_S - P_V) T_S}{(268.9 \times 10^3 - P_S)} \right]^{1/3} \quad \text{(A-9)}$$

Radiative heat transfer coefficient

$$h_{R,CS} = \sigma \Phi \frac{T_C^{\,4} - T_{SKY}^{\,4}}{T_C - T_{SKY}}, h_{R,SV}, h_{R,MD}, h_{R,RB} \quad \text{(A-10)}$$

Evaporative heat transfer coefficient in basin still

$$h_{E,SV} = 16.273 \times 10^{-3} h_{C,SV} \times \frac{P_S - P_V}{T_S - T_V}$$
$$h_{E,MD} = D \frac{\pi}{R_C T_{AV}} \frac{1}{(\delta / e^{3.6} + z)} \frac{P_M - P_D}{P_{BM}} \quad \text{(A-11)}$$

Overall heat transfer coefficient

$$\frac{1}{U_{VC}} = \frac{\ell_V}{k_V} + \frac{\ell_C}{k_C}, U_{PS}, U_{PM}, U_{DR} \quad \text{(A-12)}$$

Saturated vapor pressure(Antoine equation)

$$P_S = \exp\left[25.317 - \frac{5144}{T_S} \right], P_V \quad \text{(A-13)}$$

References

[1] M.A.S. Malik, G.N. Tiwari, A. Kumar and M.S. Sodha, Solar Distillator, Pergamon Press, Oxford, 1982.
[2] J.A. Duffie and W.A. Beckman, Solar engineering of thermal processes, Wiley, USA, 1991.
[3] G.N. Tiwari and A.K. Tiwari, Solar Distillation Practice for Water Desalination Systems, Anshan publisher, New Delhi, 2008.
[4] E.S. Fath. Desalination 116 (1998) 45–56.
[5] M.F.A. Goosen, S.S. Sabani, W.H. Shayya, C.Paton and H.Al-Ninai. Desalination 129 (2000) 63–89.
[6] K.W. Lawson and D.R. Lloyd. J. Membr. Sci. 124 (1997) 1–25.
[7] A.M. Alklaibi and N. Lior Desalination 171 (2004) 111–131.
[8] B.V. Bruggen and C. Vandecasteele. Desalination 143 (2002) 207–218.
[9] P.A. Hogan, Sudjito, A.G. Fane and G.L. Morrison. Desalination 81 (1991) 81–90.
[10] J. Koschikowski, M. Wieghaus and M. Rommel. Desalination 156 (2003) 295–304.
[11] Z. Ding, L. Liu, M.S. El-Bourawi and R. Ma. Desalination 172 (2005) 27–40.
[12] H.J. Zwijnenberg, G.H. Koops and M. Wessling. J. Membr. Sci. 250 (2005) 235–246.
[13] E. El-Zanati and K.M. El- Khatib Desalination 205 (2007) 15–25.
[14] K. Murase, H. Tobata, M. Ishikawa and S. Toyama. Desalination 190(2006) 137–146.
[15] K. Murase, Y. Yamagishi, Y. Iwashita and, K. Sugino. Int. J. Energy (in press).
[16] A.M. Alklaibi and N. Lior J. Membr. Sci. 255 (2005) 239–253.
[17] R.V. Dunkle. Proc. 1961 ASME Int. Heat Transfer Conf. 895 (1961) 119, ASME (1992).
[18] R.W. Schofield, A.G. Fane and C.J.D. Fell. J. Membr. Sci. 33 (1987) 299–313.
[19] S. Kimura and S. Nakao J. Membr. Sci. 33 (1987) 285–298.
[20] G.L. Liu, C. Zhu, C.S. Cheung and C.W. Leung. Heat Mass Transf. 34 (1998) 329–335.
[21] S. Bouguecha, R. Chouikh and M. Dhahbi. Desalination 152 (2002) 245–252.
[22] R. Chouikh, S. Bouguecha and M. Dhahbi. Desalination 181 (2005) 257–265.
[23] A.M. Alklaibi and N. Lior J. Membr. Sci. 255 (2005) 239–253, 282 (2006) 362–39.
[24] S. Toyama, T. Aragaki, H.M. Salah, K. Murase and M. Sudo. J. Chem. Eng. Japan 20 (1987) 473–478.
[25] K. Murae, S. Komiyama, A. Ikeya and Y. Frukawa. Bull. Soci. Water Sci. Japan 54 (2000) 30–36.
[26] H. Kurokawa, H.Y. Koseki, A. Yamada, K. Ebara and S. Takahashi. Kagaku Kogaku Ronbunshu 14 (1988) 330–336.